Brainstem prolactin-releasing peptide contributes to cancer anorexia-cachexia syndrome in rats

Navarro I Batista, Keila ; Schraner, Marissa ; Riediger, Thomas

Abstract: p to 80% of cancer patients are affected by the cancer anorexia-cachexia syndrome (CACS), which leads to excessive body weight loss, reduced treatment success and increased lethality. The area postrema/nucleus of the solitary tract (AP/NTS) region emerged as a central nervous key structure in this multi-factorial process. Neurons in this area are targeted by cytokines and signal to downstream sites involved in energy homeostasis. NTS neurons expressing prolactin-releasing peptide (PrRP) are implicated in the control of energy intake and hypothalamus-pituitary-adrenal (HPA) axis activation, which contributes to muscle wasting. To explore if brainstem PrRP neurons contribute to CACS, we selectively knocked down PrRP expression in the NTS of hepatoma tumor-bearing rats by an AAV/shRNA gene silencing approach. PrRP knockdown reduced body weight loss and anorexia compared to tumor-bearing controls treated with a non-silencing AAV. Gastrocnemius and total hind limb muscle weight was higher in PrPR knockdown rats. Corticosterone levels were increased in the early phase after tumor induction at day 6 in both groups but returned to baseline levels at day 21 in the PrRP knockdown group. While we did not detect significant changes in gene expression of markers for muscle protein metabolism (MuRF-1, myostatin, mTOR and REDD1), mTOR and REDD1 tended to be lower after disruption PrRP signalling. In conclusion, we identified brainstem PrRP as a possible neuropeptide mediator of CACS in hepatoma tumor-bearing rats. The central and peripheral downstream mechanisms require further investigation and might involve HPA axis activation.

DOI: https://doi.org/10.1016/j.neuropharm.2020.108289

Neuropharmacology 180 (2020) 108289

Contents lists available at ScienceDirect

Neuropharmacology

journal homepage: www.elsevier.com/locate/neuropharm

Brainstem prolactin-releasing peptide contributes to cancer anorexia-cachexia syndrome in rats

Keila Navarro I Batista, Marissa Schraner, Thomas Riediger *

University of Zurich, Institute of Veterinary Physiology, Zurich, Switzerland

ARTICLE INFO

Keywords:
undernutrition
Muscle wasting
Hindbrain

ABSTRACT

Up to 80% of cancer patients are affected by the cancer anorexia-cachexia syndrome (CACS), which leads to excessive body weight loss, reduced treatment success and increased lethality. The area postrema/nucleus of the solitary tract (AP/NTS) region emerged as a central nervous key structure in this multi-factorial process. Neurons in this area are targeted by cytokines and signal to downstream sites involved in energy homeostasis. NTS neurons expressing prolactin-releasing peptide (PrRP) are implicated in the control of energy intake and hypothalamus-pituitary-adrenal (HPA) axis activation, which contributes to muscle wasting. To explore if brainstem PrRP neurons contribute to CACS, we selectively knocked down PrRP expression in the NTS of hepatoma tumor-bearing rats by an AAV/shRNA gene silencing approach. PrRP knockdown reduced body weight loss and anorexia compared to tumor-bearing controls treated with a non-silencing AAV. Gastrocnemius and total hind limb muscle weight was higher in PrPR knockdown rats. Corticosterone levels were increased in the early phase after tumor induction at day 6 in both groups but returned to baseline levels at day 21 in the PrRP knockdown group. While we did not detect significant changes in gene expression of markers for muscle protein metabolism (MuRF-1, myostatin, mTOR and REDD1), mTOR and REDD1 tended to be lower after disruption PrRP signalling. In conclusion, we identified brainstem PrRP as a possible neuropeptide mediator of CACS in hepatoma tumor-bearing rats. The central and peripheral downstream mechanisms require further investigation and might involve HPA axis activation.

1. Introduction

The cancer anorexia-cachexia syndrome (CACS) is a severe wasting disorder caused by an ongoing and involuntary loss of body weight that cannot be fully reversed by conventional nutritional support. Characterized by loss of appetite (anorexia), skeletal muscle mass and adipose tissue (cachexia), this multifactorial syndrome is a major health concern. Depending on the type of cancer, up to 80% of patients in an advanced stage of cancer suffer from CACS (Gullett et al., 2011; Sadeghi et al., 2018). The clinical management of CACS continues to be limited because no drugs have been specifically approved for the treatment of CACS (Sadeghi et al., 2018). An increase in cytokines (e.g. TNF-α, interleukins, growth differentiation factor 15, etc.) plays a role for most of the underlying pathological mechanisms. Cytokines released from cells of the immune system or by the tumor itself act on the brain and in peripheral tissues to induce anorexia as well as endocrine and metabolic dysfunction (Langhans, 2004; Mcnamara et al., 1992). The area postrema/nucleus of the solitary tract (AP/NTS) region located in the caudal hindbrain plays a pivotal role as a target area for humoral mediators of CACS. Not only the AP but also part of the NTS lack a functional blood-brain-barrier (Broadwell and Sofroniew, 1993), which makes neurons in these areas accessible by blood-borne signalling molecules. The AP/NTS region mediates physiological satiation induced by the satiation hormones amylin and CCK leading to an inhibition of energy intake (see (Riediger, 2012; Lutz, 2010) for review). AP-lesioned rats are partly protected against CACS (Borner et al., 2017) and TNF-α-induced anorexia (Bernstein et al., 1991). We recently identified the brainstem neuropeptide GLP-1 (glucagon-like peptide-1) as mediator of CACS. Pharmacological and genetic disruption of hinbrain GLP-1 signalling attenuated anorexia and cachectic body weight loss in hepatoma tumor-bearing rats (Borner et al., 2018). However, GLP-1 might not be the only neuropeptidergic mediator of CACS in the brainstem (see Figs. 2–5).

Prolactin-releasing peptide (PrRP) is also expressed in NTS neurons. While GLP-1 is produced by glutamtergic neurons (Zheng et al., 2015), PrRP neurons are noradrenergic and belong to the A2 subpopulation in

* Corresponding author.
E-mail address: triedig@vetphys.uzh.ch (T. Riediger).

https://doi.org/10.1016/j.neuropharm.2020.108289
Received 17 April 2020; Received in revised form 5 August 2020; Accepted 25 August 2020
Available online 2 September 2020

the NTS (Maniscalco et al., 2015; Roland et al., 1999). There is evidence for an involvement of PrRP in the control of food intake and energy balance. Mice deficient for PrRP or its receptor GPR10 become obese and lipidized analogs of PrRP counteract experimentally induced obesity (Mochiduki et al., 2010; Gu et al., 2004; Maletínská et al., 2015). Accordingly, mice treated with a PrRP-specific antibody show hyperphagia (Takayanagi et al., 2008), but no studies investigated the role of PrRP in CACS. In addition to a possible involvement in cancer anorexia, PrRP might increase glucocorticoid-dependent muscle wasting under cancer conditions.

Stress hormone signalling contributes to cachexia and is triggered via neuronal pathways originating in the hindbrain. Projections from the NTS mediate hypothalamus-pituitary-adrenal (HPA) axis activation involving a stimulation of neurons in the hypothalamic paraventricular nucleus (PVN). Under chronic disease conditions (e.g. cancer, chronic infection, etc.) HPA axis activation leads to excessive muscle wasting (see (Burfeind et al., 2016; van Norren et al., 2017; Braun and Marks, 2015) for review). PrRP/A2 neurons are synaptically connected to neurons of the PVN expressing corticotropin-releasing hormone (CRH) (Liposits et al., 1986). Moreover, PrRP and noradrenaline stimulate neuronal activity in the PVN and increase ACTH and corticosterone plasma levels (Seal et al., 2002; Mera et al., 2006; Cole and Sawchenko, 2002). Glucocorticoids increase protein breakdown and decrease protein synthesis (Schakman et al., 2013). The E3 ubiquitin ligase muscle RING finger protein-1 (MuRF-1) is one of the mediators of glucocorticoid-dependent muscle wasting (Bodine and Baehr, 2014). MuRF-1 deficient mice are protected against muscle degradation induced by synthetic glucocorticoids (Baehr et al., 2011). Glucocorticoids also upregulate the expression of myostatin (Allen and Loh, 2011), which inhibits muscle growth and differentiation via MuRF-1 signalling (Taylor et al., 2001; Gilson et al., 2007). Muscle protein synthesis depends on the mTOR (mammalian target of rapamycin) pathway (Saxton and Sabatini, 2017). Anabolic mTOR signalling is inhibited by the mTOR suppressor gene REDD1 (Wang et al., 2006).

Given their role in energy homeostasis and stress hormone signalling, PrRP neurons may be involved in anorexia, muscle wasting and HPA axis activation under cancer conditions. To explore this, we knocked down PrRP expression in the NTS of rats using a shRNA gene silencing approach. We measured food intake, body weight development, muscle mass, corticosterone levels, and markers for muscle protein degradation and synthesis.

2. Material and methods

2.1. Animals and housing conditions

Male Buffalo rats (Charles River Laboratory, USA) weighing 410–480 g were single housed in wire-mesh cages. Exposed to a 12-h artificial life cycle (lights on at 6:00 a.m.) and a controlled temperature (21 ± 1°C), the animals had ad libitum access to standard laboratory chow. All animal procedures were approved by the Veterinary Office of the Canton of Zurich (license number: 042/2018).

2.2. PrRP gene knockdown in the NTS by adeno-associated virus

Capsid 8 adeno-associated viruses (AAV) with a physical titer of 4.1×10^{12} vg/ml were designed and produced by the Viral Vector Facility at the University of Zurich. The control virus encoded four identical non-target sequences of short-hairpin RNA (shRNA) under the control of the human synapsin-1 promoter hSyn1. The vector used for the knockdown group induced the expression of four different shRNA constructs directed against the PrRP gene, also under the control of hSyn1. In addition, both of the vectors' genomes contained enhanced green fluorescent protein (EGFP) as a reporter gene to allow the confirmation of successful transfection and expression of the vectors' genome in cells of the target area. The non-silencing shRNA construct designed for the control AAV was 63 base pairs long and did not target any known gene (atctcgcttgggcgagagtaagtagtgaagccacagatgtacttactctcgcccaagcgagag). The AAV used for the knockdown group contained four different anti-PrRP sequences of 22 base pairs (first: tagcagcagcaagcacagaagc, second: caagcttagcagcagcaagcac, third: gtctccatggagtgctggtggg, fourth: aagtccagtgacatccctcggg). Rats were randomly divided into two different experimental groups, one treated with the AAV containing the non-silencing shRNA (control-AAV) and the other treated with the AAV containing the anti-PrRP shRNA sequences (PrRP-AAV) on day −23.

2.3. Stereotaxic surgery

Rats were deeply anaesthetized with a mixture of ketamine (Streuli Pharma; Switzerland; Ketanarkon; 40 mg/kg) and medetomidine (Virbac; UK; Medetor; 80 mg/kg) injected intraperitoneally. The animals also received the antibiotics enrofloxacin (Bayer; Germany; Baytril; 0.4 mL/kg; injected subcutaneously) and the analgesic meloxicam (Boehringer Ingelheim; Germany; Metacam; 1 mg/kg; injected subcutaneously). Surgical anaesthesia was confirmed via the loss of toe pinch withdrawal reflex. Afterwards, the animals' heads were shaved and fixed to a stereotaxic frame (Stoelting, USA). Body temperature was monitored throughout the surgery and a heating pad was used to minimize anaesthesia-induced heat loss. Once the head was put in a ventroflexed position, a midline incision was made above the occipito-atlantal joint and the underlying muscles were retracted. The occipito-atlantal membrane was removed in order to expose the area of the obex, which was used as a reference point for the stereotactic injection into the NTS. A microinfusion pump (World Precision Instrument, USA) was assembled into a stereotaxic arm and equipped with a 10 µl glass-syringe (Nanofil, World Precision Instrument, USA) and a 35G bevelled needle (World Precision Instrument, USA). The needle was moved to a position 100 µm caudal and 400 µm lateral to the obex and then lowered 600 µm starting from the surface of the brain in order to inject into the medial portion of the NTS (mNTS). These injection sites were chosen based on the location of PrRP neurons (Roland et al., 1999) and correspond to bregma −14.52 mm according to the rat brain atlas by Paxinos and Watson (2007). Two µl of AAV were bilaterally infused into the mNTS (1 µl per side) at a speed of 0.2 µl per minute. Injection volume and speed were controlled with a Micro 4 Microsyringe Pump Controller (World Precision Instrument, USA). After infusion was completed, the needle was kept at the site of injection for 2 min to prevent reflux. After the injection, the retracted muscles and skin were sutured. Anaesthesia was reversed with the α_2 adrenoceptor antagonist atipamezole hydrochloride (Virbac; UK; Revertor; 0.7 mg/kg). For the post-operative care, Medetor and Baytril were administered 24 h and 48 h after surgery.

2.4. Confirmation of adeno-associated virus infection in the NTS

Before carrying out any of the experiments described below, two Buffalo rats were injected with the control virus. After a recovery period of three weeks, the animals were euthanized and perfused. The rats were anaesthetized with pentobarbital (100 mg/kg, intraperitoneal). Perfusion pressure was generated by gravity (1.5 m hydrostatic pressure). Perfusion with phosphate-buffered saline (PBS) was conducted for 2 min before fixing the tissues with 4% paraformaldehyde perfusion for 4 min. Brains were removed and postfixed in 4% paraformaldehyde for 24 h at 4 C and transferred to 20% sucrose for overnight cryoprotection. Brains were cut in 20 µm thick coronal slices using a cryomicrotome. The sections were mounted, air-dried for 7min and rehydrated for 15min in PBS. After coverslipping, the slides containing the NTS were analysed under a fluorescent microscope (Imager.Z2, Zeiss, Germany) in order to identify EGFP expression, which served as an indicator of successful transfection.

2.5. Cell culture and tumor model

Morris hepatoma 7777 cells (McA-RH7777, Catalogue No. CRL-1601, ATCC, USA) were cultured at 37°C and 5% CO_2, in a media (DMEM, Catalogue No. 30–2002, ATCC, USA) supplemented with 10% fetal bovine serum and 1% penicillin-streptomycin. Subcultivation was performed weekly, before 70% confluence was reached. Petri dishes were washed with DMEM to detach adhered cells, which were then transferred into a falcon tube and centrifuged at 850 rpm for 10min. The resulting cell pellet was resuspended in fresh growth media in a 1:4 ratio. Tumor induction was performed three weeks after surgery. Cancer cells were centrifuged and resuspended in PBS. Once their viability was confirmed via the trypan blue exclusion method, 10^7 viable cells in 250 μl of PBS were subcutaneously inoculated per rat, between the shoulder blades with a 20G needle. To achieve an accurate injection, the rats were shortly anaesthetized with isoflurane. The experiment was terminated when our criteria defining the humane endpoint for tumor-bearing animals were reached.

2.6. Monitoring of body weight and food intake

Body weight and food intake were measured on a daily basis at 10:00 a.m. during the light phase. Food intake was calculated by subtracting the total weight of spilling resistant food hoppers from the weight measured on the previous day.

2.7. Confirmation of PrRP gene knockdown

PrRP transcripts were measured in all experimental animals at the end of the experiment. After the injection of a lethal dosage of pentobarbital (100 mg/kg, intraperitoneal) rats were decapitated, and the brains collected and preserved in dry ice until their storage in the −80°C freezer. In the cryomicrotome (Leica Microsystem, Germany), micropunches of the NTS and the primary somatosensory cortex were obtained using a 2 mm micropuncher (Soft Tissue Biopsy Punch, Zivic Instruments, USA). The cortex area corresponded to the coordinates bregma −1.30 mm, lateral 5 mm and dorsoventral 2 mm according to the rat brain atlas (Paxinos and Watson, 2007) and was used as a negative control as it lacks PrRP neurons (Roland et al., 1999).

RNA was extracted and purified from each tissue punch according to the manufacturer's instructions (Reliaprep, Promega, USA) and quantified using the spectrophotometer (NanoDrop, 2000; Thermo Fischer Scientific, USA). The extracted RNA was reverse transcribed to cDNA using the SensiFAST cDNA Synthesis Kit (Bioline, UK). Fast quantitative real-time PCR using pre-designed Taqman probes (Applied Biosystems, USA) was performed. Rps18 (Rn01428915) was used as housekeeping reference gene to quantify gene expression in the brain tissue. The knockdown was analysed using Rn00573653 probe to amplify PrRP transcripts. Given that vector-induced inflammation might be associated with reduced transgene expression as well as altered neuronal function (Ahi et al., 2011), the presence of inflammatory biomarkers in the NTS was evaluated using the probes TNF-α (Rn01525859), IL-1β and IL-6 (probes designed by Dunn-Meynell et al. (2016)). Cortical samples were also included in the analysis as negative controls.

2.8. Gene expression in muscle tissue

After sacrifice, the left gastrocnemius, anterior tibialis, and soleus muscle were dissected, weighed, flash-frozen in liquid nitrogen and stored at −80°C. Skeletal muscle MuRF-1 gene expression was assessed using the digital droplet PCR (ddPCR). 30 μl of RNA were isolated from 15 to 20 mg of muscle tissue, analysed in the spectrophotometer and later diluted with nuclease-free water to ensure even concentration (18 ng/μl) across samples for the conversion into cDNA by reverse transcription. All procedures were performed using the kits described above for the preparation of the brain micropunches. The first step of ddPCR was droplet generation, which consisted of the samples' fractioning into nanometric oil droplets. For this, 10 μl of cDNA (0.1 ng/l) were combined with 10 μl of ddPCR Supermix and 1 μl of 20× Taqman assay (Rn00590197) according to the instructions of the manufacturer (QX100 Droplet Generator, BioRad, USA). In order to amplify the samples' cDNA, endpoint PCR was performed using the Mastercycler (Eppendorf; Germany). QX100 Droplet Reader (BioRad, USA) quantified the amount droplets positive for MuRF-1. ddPCR data was analysed with QuantaSoft Software. Further analysis of muscle gene expression in gastrocnemius was performed by qPCR with GAPDH (Rn01775763) as housekeeping reference gene. The following probes were used to assess the muscle degradation marker myostatin (Rn00569683), the marker for suppression of mTOR REDD1 (Rn01433735) as well as mTOR itself (Rn00693900).

2.9. Measurement of corticosterone

Blood samples (approx 250 μl) from the lateral tail vein were collected by tail nicking one day before tumor cell inoculation (day −1), a week afterwards (day 6) and at the end of the experiment (day 21), always at 10:00 a.m., i.e. 4 h after light onset. For this, 500 μl EDTA-coated tubes, previously prepared with 1 μl of protease inhibitor, were employed. Immediately after blood collection, all samples were centrifuged at 12,000 rpm and 4°C for 10 min in order to separate plasma from blood cells. Plasma corticosterone levels were measured using the DetectX Corticosterone Enzyme Immunoassay Kit (Arbor Assays, USA). The ELISA plates were analysed in a microplate reader (Epoch 2, BioTek, USA) at 450 nm.

2.10. Data evaluation and statistical analysis

All data are expressed as mean ± standard error of the mean. Quantitative PCR data were analysed with the delta-delta Ct method, which normalizes the cycle threshold values of the gene of interest against those of the housekeeping gene. PrRP, TNF-α, IL-1β and IL-6 expression (relative to Rps18) were calculated and compared between PrRP-AAV and control-AAV animals.

To assess body weight changes associated with CACS, two calculations were performed. First, body weight before tumor induction (day −1) was subtracted from weight at day 13, which corresponded to the onset of body weight loss. For the second, body weight on day 13 was subtracted from weight before sacrifice (day 20). The latter period corresponded to the phase of apparent cachexia. Due to a body weight difference between the experimental groups, individual food intake values were corrected for body weight (food intake/100 g body weight). In addition, average daily food intake per week was calculated for each rat over the 3-week period following tumor cell inoculation.

Unpaired student's T-test (two-sided) was employed to compare differences between two groups. P values were corrected for false discovery rate for multiple tests between two groups. For multiple comparisons, a one-way ANOVA or repeated measures one-way ANOVA in combination with a Tukey's multiple comparison test was applied. In all statistical tests, a p value lower than 0.05 was considered significant. Data analysis was performed using Graphpad Prism 8.

3. Results

3.1. Knockdown of PrRP gene expression in the brainstem

Fig. 1A illustrates the approximate injection sites at the level of the NTS. As confirmed by the expression of EGFP, transfection occurred in the diffusion field of the AAV, which was spatially restricted to the dorsomedial part of the medulla oblongata (1 B). Animals injected with PrRP-AAV showed a significant 96 ± 2% knockdown of PrRP gene expression compared to animals receiving control-AAV (1C). To exclude local inflammatory responses, we assessed expression of TNF-α, IL-1β

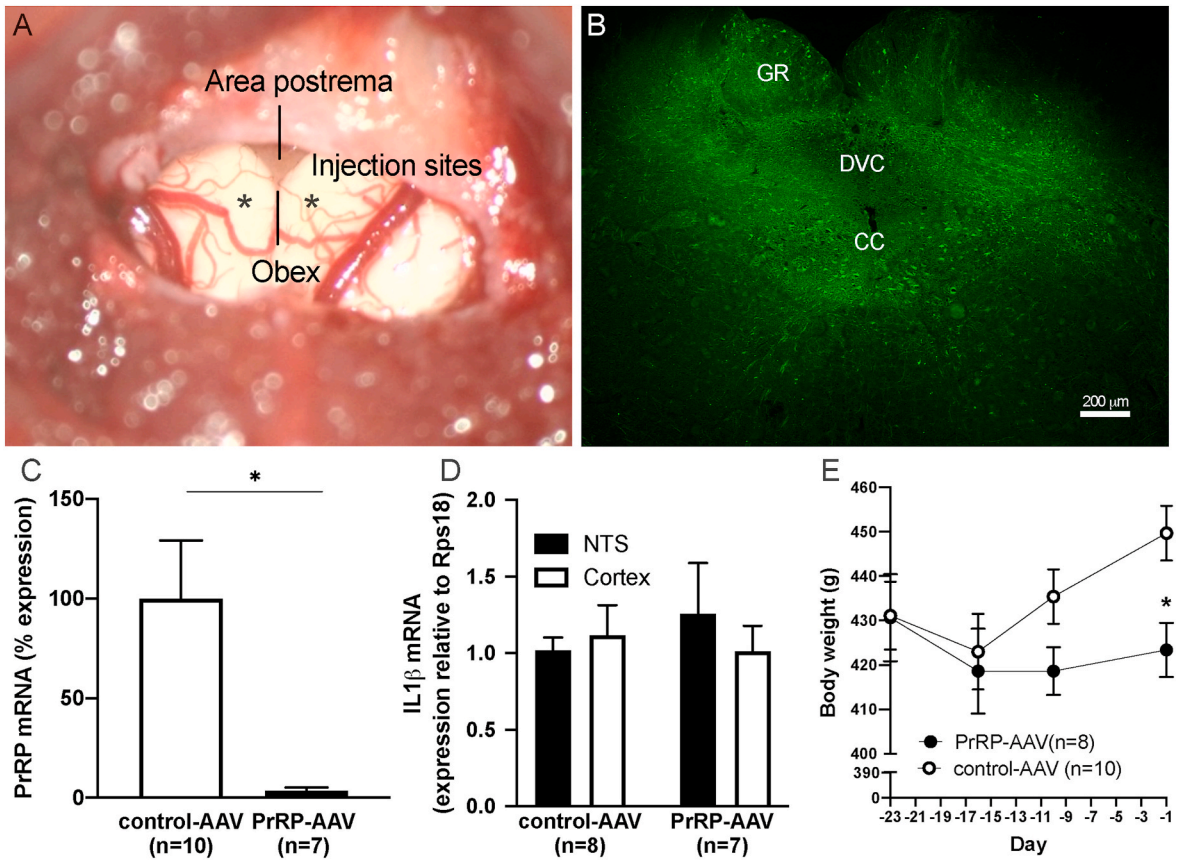

Fig. 1. PrRP knockdown in the NTS. A) Top view of surgery field illustrating the position of the AAV injection sites. B) Distribution of EGFP expression in the medulla oblongata reflecting successful AAV transfection (GR, nucleus gracilis; DVC, dorsal vagal complex; CC, central canal). C) PrRP expression was effectively reduced in PrRP-AAV rats. D) AAV injection into the NTS did not affect the local expression of the inflammatory marker IL1-β when compared to expression levels in the cortex. E) Body weight development after AAV injection (day −23) under non-tumor conditions. * $p \leq 0.05$ Student's T-test.

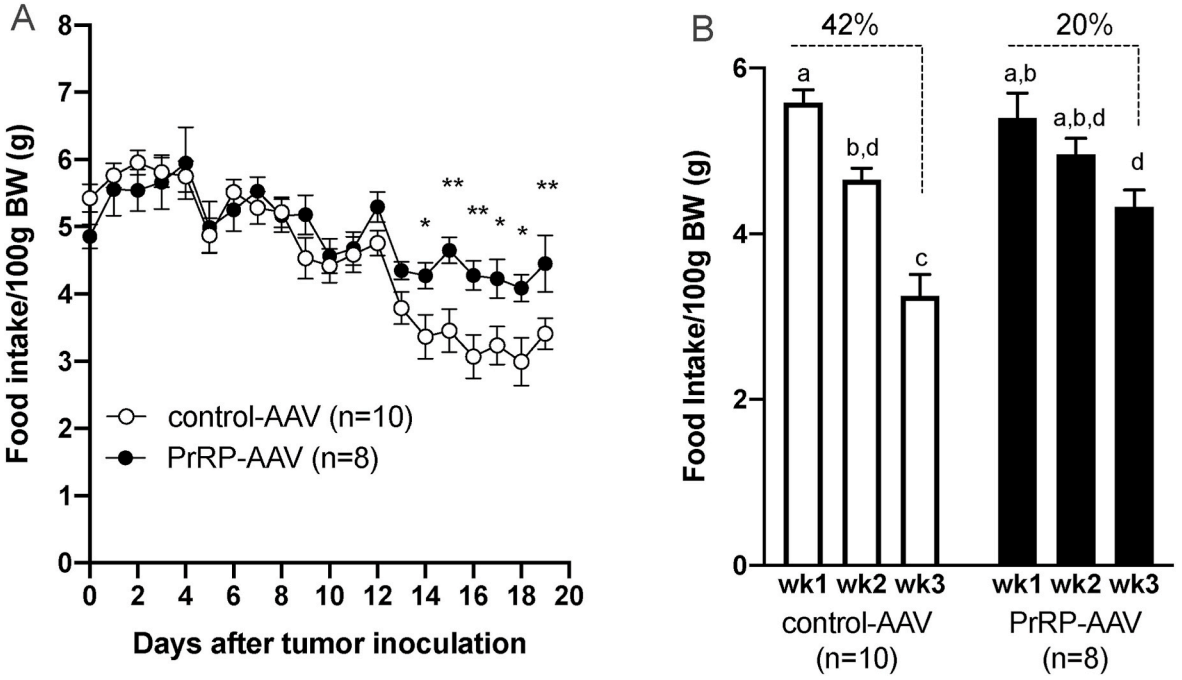

Fig. 2. PrRP knockdown in the NTS attenuated cancer-induced anorexia. A) Mean daily food intake corrected for body weight (BW) was significantly higher in PrRP-AAV rats compared to controls during the last week of tumor growth. B) The mean individual food intake averaged across weeks significantly decreased about twice as much in control animals compared to PrRP-AAV rats. * $p \leq 0.05$; ** $p \leq 0.01$ Student's T-test; different letters indicate significant differences, one-way ANOVA with Tukey's multiple comparison test, $p \leq 0.05$.

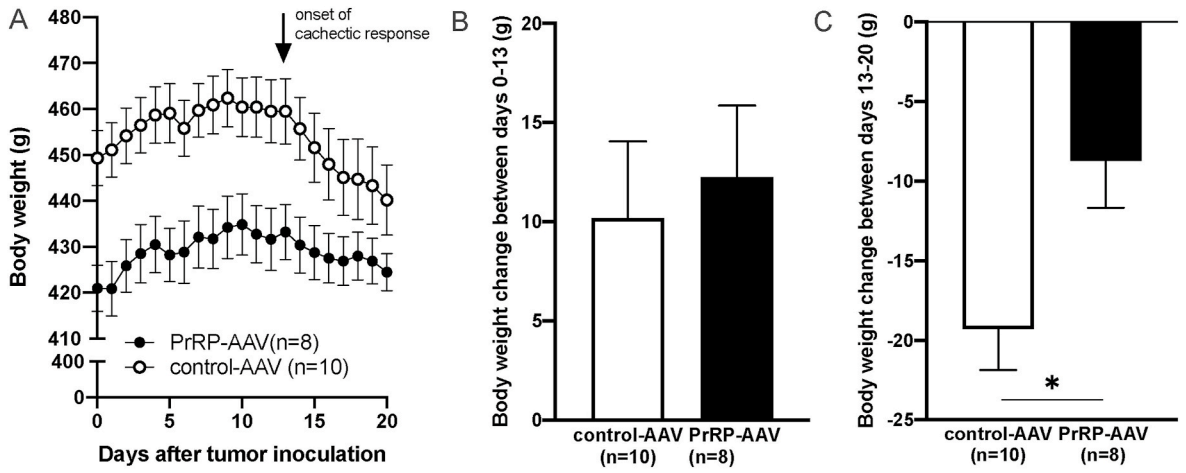

Fig. 3. PrRP knockdown in the NTS attenuated cancer-induced body weight loss. A) Body weight development in PrRP-AVV and control rats after inoculation of hepatoma tumor cells. B/C) While both experimental groups showed similar body weight gain during the first two weeks of tumor growth, both groups lost body weight in the last week. However, body weight loss was significantly reduced in PrRP-AVV rats. * $p \leq 0.05$, Student's T-test.

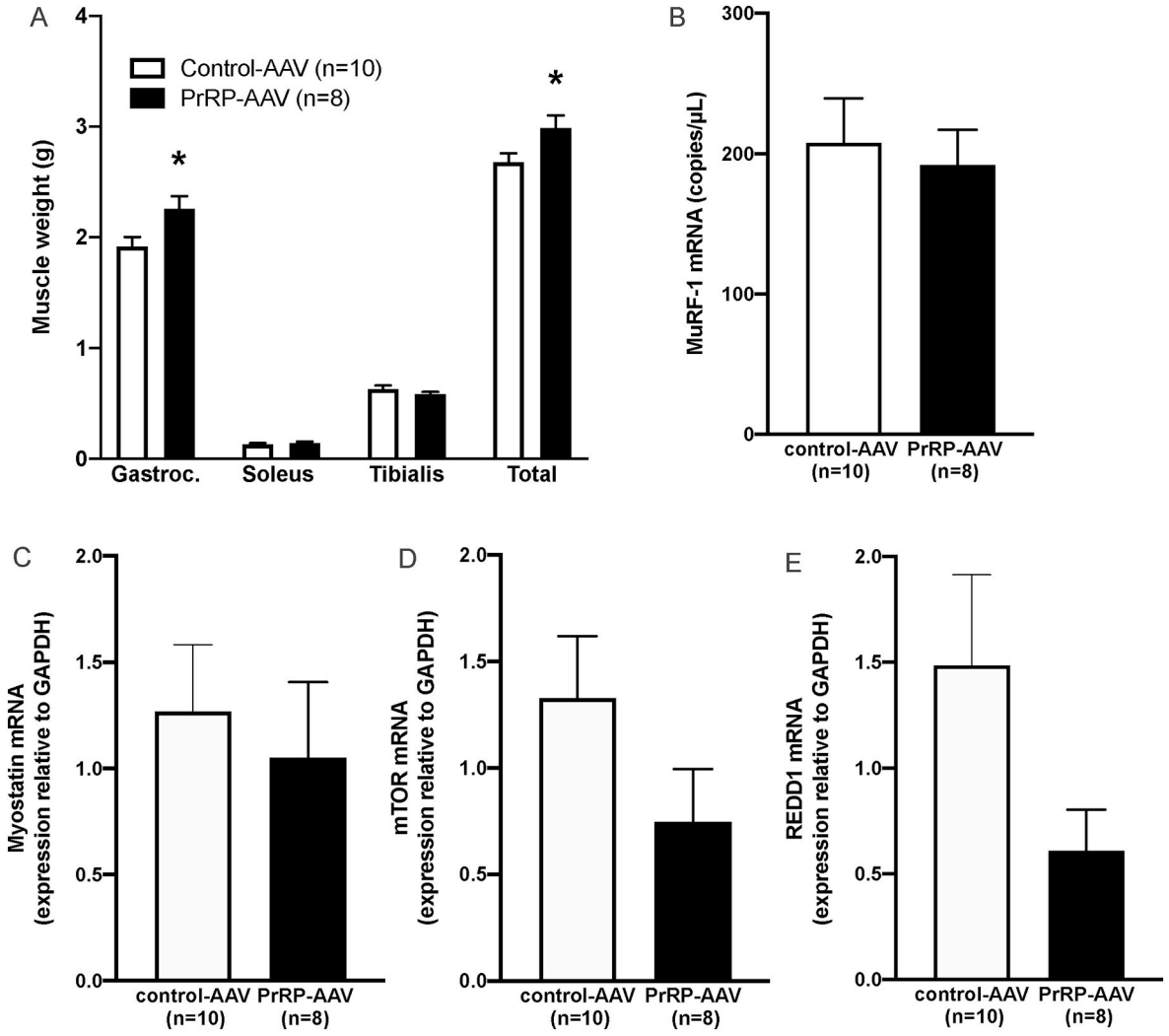

Fig. 4. PrRP knockdown in the NTS attenuated cancer-induced muscle wasting. A) Knockdown of PrRP in the NTS resulted in higher hindlimb muscle mass. B/C) Muscle atrophy markers MuRF-1 and myostatin were not affected by the knockdown of PrRP. D/E) mTOR and REDD1 expression tended to be lower in PrRP-AAV group. * $p \leq 0.05$, Student's T-test.

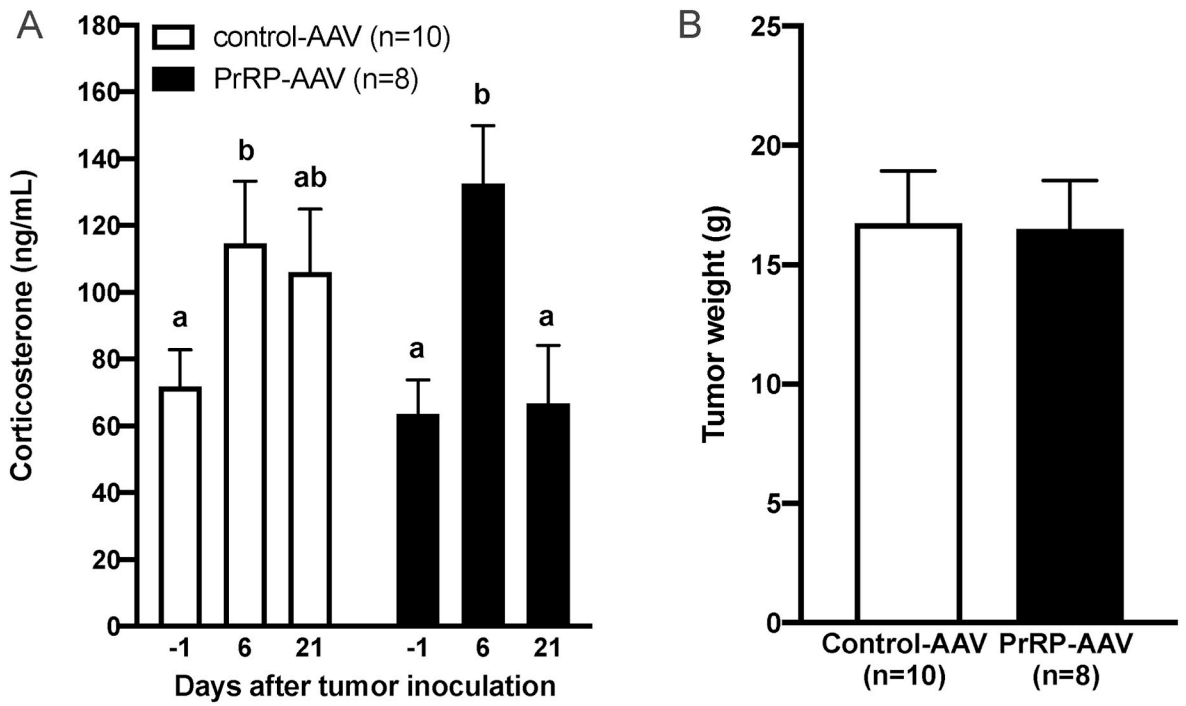

Fig. 5. Corticosterone levels and tumor size. A) Both groups showed increased corticosterone levels at day 6 after tumor cell inoculation compared to baseline levels (day −1). In PrRP-AAV rats corticosterone levels significantly decreased between day 6 and day 21 and returned to baseline levels. B) Tumor weights were not affected by PrRP knockdown. Different letters indicate significant intra-group differences; repeated measures one-way ANOVA with Tukey's multiple comparison test, $p \leq 0.05$ (A). Student's T-test (B).

and IL-6 expression at the injection site in the NTS and in the cerebral cortex, which was used as a negative control. In control-AAV and PrRP-AAV rats, the three inflammatory markers had similar expression values in the NTS and in the cortex (see 1D for IL-1β, TNFα and IL-6 not shown). Hence, there was no indication of local inflammation induced by the viral vector. Both groups had almost identical average body weight at the time point of AAV injection (day −23). After recovery from surgery, body weight development started to diverge. At day −1 control rats were on average 26 g heavier than PrRP knockdown animals which was significant (1 E).

3.2. Brainstem PrRP contributes to cancer anorexia and body weight loss

In line with our previous publications (Borner et al., 2017, 2018), tumor-bearing rats decreased food intake after inoculation with hepatoma cells. When corrected for differences in body weight, food intake of PrRP knockdown rats was similar to control rats during the first two weeks but significantly higher during the last week of the experiment (2 A). Daily food intake averaged across each of the three experimental weeks progressively and significantly decreased by 42% in the control-AAV group whereas PrRP-AAV rats consumed only 20% less in the third compared to the first week after tumor cell inoculation (2 B). After induction of tumor growth, control and knockdown rats showed a similar body weight development during the first two weeks. Control rats continued to be heavier (3 A) but this difference in body weight was not significant. The average body weight converged mainly because of a higher weight loss in the control rats. Between days 0 and 13 both groups gained a similar amount of weight. While both groups lost weight during the last week, the average body weight loss in controls was significantly higher and twice as much as in PrRP-AAV rats during week 3 (3 B–C). Hence PrRP knockdown rats were partly protected against cachexia.

3.3. Brainstem PrRP mediates cancer-induced muscle wasting

Disruption of hindbrain PrRP signalling resulted in higher muscle mass at study end. Gastrocnemius and total muscle mass was significantly higher in PrRP-AVV rats compared to controls while we did not observe significant differences in soleus and tibialis muscle weights (4 A). Despite this effect of PrRP gene silencing on muscle wasting there were no significant differences in gene expression of MuRF-1, mTOR, myostatin, and REDD1 between the groups (4 B-E). However, REDD1 and mTOR expression tended to be lower in PrRP-AAV rats (student's T-test, $p = 0.105$ and $p = 0.162$, respectively). Interestingly, corticosterone levels were increased significantly at day 6 after tumor cell inoculation in both groups. However, only in PrRP knockdown rats did the elevated corticosterone levels return to the baseline level measured before tumor growth. In the control group, corticosterone appeared to remain elevated until the end of the experiment, although the levels at day 21 did not reach significance when compared to baseline values (5 A). Differences in tumor burden did not seem to account for any of the observed differences in the experimental parameters because average tumor weights were almost identical in both groups (5 B).

4. Discussion

This study sought to determine whether PrRP contributes to cancer anorexia and body weight loss in a rat model for AP/NTS dependent CACS. (Borner et al., 2017). We developed a highly effective shRNA/AAV gene silencing approach to knockdown PrRP expression in the NTS. We analysed changes in body weight and food intake, muscle mass, stress hormone levels, and muscle markers reflecting muscle protein degradation and synthesis. Overall, our findings indicate that genetic disruption of the PrRP signalling in the NTS significantly ameliorates CACS.

PrRP gene silencing was remarkably effective, which appears to be due to the AAV's highly effective plasmid design with the inclusion of four different shRNA sequences (Taxman et al., 2010). There were no

indications of local inflammation, which is in favor of a high knockdown efficiency (Nayak and Herzog, 2010) without the risk of confounding side effects. As confirmed histologically, the transfection was restricted to the dorsomedial medulla oblongata covering the area of the NTS where PrRP expressing neurons are located (Lee et al., 2000; Roland et al., 1999). Therefore, it is unlikely that our AAV knockdown approach affected PrRP expression in other brain areas, although we did not specifically analyze this.

The PrRP knockdown considerably attenuated body weight loss during the phase of cachexia even though the absolute body weight was not different between the groups at the end of the experiment. This was obviously due to the higher body weight gain of the AAV-control rats before tumor cell inoculation. The attenuation of cachexia in the PrRP-AVV group is reflected by a mitigation of tumor-induced body weight loss rather than by a difference in absolute body weight per se. Presumably, the absolute body weight of the tumor-bearing controls would decrease below the level of the knockdown rats at a later stage, but the experimental duration in cancer models is limited because of rapid tumor progression and the requirement to establish humane endpoints. While there is no clear definition for cancer cachexia in animal models, weight loss rather than absolute body weight is a key parameter in the definition of cachexia in humans (Fearon et al., 2011; Vanhoutte et al., 2016). We therefore believe it is justified to interpret the attenuation of body weight loss together with our other findings as an amelioration of CACS by the knockdown of PrRP. It appears plausible based on our findings that PrRP acts as a causal mediator of CACS, but we cannot rule out the possibility that the knockdown of PrRP counteracts CACS without direct involvement in the underlying pathological processes. However, this would imply that the knockdown per se induced an anabolic effect when CACS developed. We did not specifically control for this, but the similar body weight gain of PrRP-AAV and control-AAV for a period of 13 days before the onset of CACS does not support the idea of an anabolic effect caused by the knockdown.

The hepatoma tumor model is characterized by anorexia, which parallels body weight loss. In our previous studies we pair-fed non-tumor-bearing and tumor-bearing rats and compared body weight development to ad libitum fed controls (Borner et al., 2017). At a similar terminal time point as in our current study, around half of the cancer-induced body weight loss appeared to be explained by decreased food intake because pair-fed rats did not lose weight to the same extent as tumor-bearing animals. Therefore, the attenuation of cancer anorexia by PrRP knockdown presumably contributed to body weight loss, but we did not reconfirm this in our current studies. Notably, food restriction might lead to the development of food-seeking behaviour and other confounding factors in pair-fed animals (e.g. changes in energy expenditure) that are difficult to control for.

PrRP-AAV rats had higher gastrocnemius and total hind limb muscle mass than the controls. Similar to our previous studies involving a knockdown of GLP-1 in the NTS (Borner et al., 2018), we did not observe significant changes in the soleus and tibialis muscle mass, which might be less susceptible to cachexia. The effect of PrRP knockdown on gastrocnemius muscle mass was not paralleled by a change in MuRF-1 mRNA levels. In C26 tumor-bearing mice, MuRF-1 is overexpressed 20 days after tumor induction (Villars et al., 2017), but not at day 15 or earlier time points. Therefore we analysed MuRF-1 expression at the end of the experiment which appeared to be the most likely time point to observe changes in expression. While we cannot rule out the possibility that MuRF-1 expression might have been altered earlier during the experiment, changes in MurF-1 expression do not seem to contribute to PrRP-dependent muscle wasting in this model. We also analysed the expression of other markers known to be involved in muscle wasting. Myostatin is an extracellular signalling peptide that negatively controls myogenesis via different intracellular pathways (Rodriguez et al., 2014). Knockdown of myostatin expression by RNA interference attenuates cancer-dependent muscle wasting (Liu et al., 2008). Given the similar myostatin expression in PrRP-AAV rats and controls, knockdown of PrRP does not seem to act through increased myostatin signalling at least with respect to the transcriptional level. Interestingly, we observed tendencies of reduced expression levels for mTOR and REDD1 in PrRP-AVV rats compared to controls, although the differences did not reach statistical significance. While some studies demonstrated reduced mTOR signalling in cancer cachexia (White et al., 2011; Puppa et al., 2014; Chen et al., 2016), other studies support the idea that mTOR inhibition counteracts cachexia by modulating mTOR-dependent autophagy (Pigna et al., 2016; Zhao et al., 2015). Notably, mTOR pathway activity is not only reflected by mTOR expression, but also by mTOR phosphorylation and the activation of the mTOR receptor complex 1 (mTORC1), which we did not directly analyze. REDD1 functions as an inhibitor of the mTORC1 (Deyoung et al., 2008). A reduced expression of REDD1 in PrRP-AAV rats might reflect increased mTOR pathway activity. Taken together, our findings may suggest some alterations of the mTOR pathway in response to PrRP knockdown, but it remains to be explored if this results in a significant change of downstream signalling processes.

At day 6 after tumor cell inoculation, corticosterone levels were elevated in both groups compared to baseline values. While in control-AAV rats corticosterone concentrations remained at a similar level on day 21, corticosterone returned to baseline levels in PrRP-AAV rats. This finding points to a PrRP-dependent increase in stress hormone signalling during cancer cachexia. It is interesting that PrRP knockdown did not prevent the early rise in corticosterone. Presumably, the mechanisms contributing to HPA axis activation during the course of tumor growth involve diverse pathways that are independent of PrRP. Injection of tumor cells per se and the host reactions during the initial phase may trigger different stressors than those caused by the increasing tumor burden at later stages.

The humoral mediators of CACS in hepatoma tumor bearing rats have not yet been clearly determined. While the typical cytokines contributing to CACS are not elevated in this tumor model (Ruud and Blomqvist, 2007), we previously reported highly elevated levels of GDF-15 (Borner et al., 2017), which acts via the recently discovered receptor GFRAL in the AP/NTS region (Emmerson et al., 2017). Thus PrRP expressing NTS neurons are well-positioned to be directly or indirectly activated by GDF15 or other humoral mediators of CACS acting on the AP/NTS region. Immunohistological studies detecting cancer-induced neuronal activation (c-Fos), and PrRP and GFRAL expression might help to shed more light on the cellular responses and neuronal phenotypes. Whether decreased corticosterone levels following PrRP knockdown contributed to the mitigation of CACS in our model requires further investigation directly targeting glucocorticoid signalling. Muscle specific knockout of the glucocorticoid receptor resulted in a 70% decrease of muscle wasting in mice bearing Lewis lung cancer tumors (Braun et al., 2013), which highlights the importance of stress hormone signalling in CACS.

To assess the effect of PrRP knockdown under non-pathological conditions, we monitored body weight development prior to tumor induction. Disruption of PrRP gene expression resulted in diverging weight gain and significantly lower body weight three weeks after AAV injections. This finding appears unexpected as most literature describes PrRP as an anorexigenic hormone with respect to its action on food intake (see (Tachibana and Sakamoto, 2014) for review). Blocking of PrRP results in hyperphagia and increased body weight. Moreover, PrRP-deficient mice and WT mice that received an injection of an anti-PrRP antibody into the lateral cerebral ventricle develop late-onset obesity (Takayanagi et al., 2008). However, these findings should be compared with caution across the studies because there are relevant methodological differences. While we only targeted PrRP expressing cells in the NTS, Takayanagi et al. used mice with a global knockdown affecting all PrRP-expressing neuronal populations, including those in the dorsomedial hypothalamus and the ventrolateral medulla (Takayanagi et al., 2008). Similarly, intracerebroventricular injection of the PrRP neutralizing antibody is likely to block central PrRP actions in a

different manner than our specific knockdown in the NTS. Irrespective of these considerations, the lower body weight gain induced by PrRP knockdown under non-tumor conditions appears surprising given its anti-cachectic effect during tumor growth. It was beyond the scope of our studies to investigate the effect of PrRP knockdown in the NTS under non-pathological conditions in more detail, but future studies using a similar approach should focus on this interesting finding. Given the role of A2 neurons in physiological satiation it would also be interesting to elucidate whether PrRP and noradrenaline might have different roles in physiological and pathological anorexia. With respect to a possible treatment approach against CACS, any effect that reduces basal body weight or body weight gain would be undesired. The reduction in body weight gain was not apparent anymore during the pre-cachectic phase on days 0–13 after tumor cell inoculation. Therefore, it is questionable whether it might represent a relevant limitation during a longer lasting therapeutic approach targeting PrRP signalling because the effect of the knockdown did not appear to be progressive.

In summary, this is the first study to explore the involvement of brainstem derived PrRP in the pathology of CACS. Our experiments point to a possible role of PrRP as a neuropeptide mediator of CACS. Disrupting PrRP signalling might be therapeutically exploited to ameliorate CACS-related symptoms and possibly HPA axis activation under cancer conditions. Given the recently demonstrated involvement of hindbrain GLP-1 in CACS (Borner et al., 2018), it would be interesting to investigate if there is an interaction between these neuropeptides, i.e. whether their actions are interdependent or if they function as mediators in discrete pathways originating in the brainstem. Future studies should also shed more light on the possible upstream and downstream mechanisms involved in PrRP-dependent CACS and validate our findings in different cancer models.

Funding sources and acknowledgments

Swiss National Science Foundation (31003A-179234).

The laboratory work was partly performed using the logistics of the Center for Clinical Studies at the Vetsuisse Faculty of the University of Zurich.

The authors gratefully acknowledge the help of the group of Dr. Jean-Charles Paterna (Viral Vector Facility, University of Zurich, ETH Zurich) for the generation of the viral vectors. We thank Prof. Dr. Thomas A. Lutz (Institute of Veterinary Physiology, University of Zurich) for the critical reading of the manuscript.

CRediT authorship contribution statement

Keila Navarro I Batista: Investigation, Writing - original draft, Visualization. **Marissa Schraner:** Investigation, Writing - original draft, Visualization. **Thomas Riediger:** Conceptualization, Supervision, Investigation, Writing - original draft, Funding acquisition.

References

Ahi, Y.S., Bangari, D.S., Mittal, S.K., 2011. Adenoviral vector immunity: its implications and circumvention strategies. Curr. Gene Ther. 11, 307–320.

Allen, D.L., Loh, A.S., 2011. Posttranscriptional mechanisms involving microRNA-27a and b contribute to fast-specific and glucocorticoid-mediated myostatin expression in skeletal muscle, American journal of physiology. Cell physiology 300, 124–137.

Baehr, L.M., Furlow, J.D., Bodine, S.C., 2011. Muscle sparing in muscle RING finger 1 null mice: response to synthetic glucocorticoids. J. Physiol. 589, 4759–4776.

Bernstein, I.L., Taylor, E.M., Bentson, K.L., 1991. TNF-induced anorexia and learned food aversions are attenuated by area postrema lesions. Am. J. Physiol. Regul. Integr. Comp. Physiol. 260, R906–R910.

Bodine, S.C., Baehr, L.M., 2014. Skeletal muscle atrophy and the E3 ubiquitin ligases MuRF1 and MAFbx/atrogin-1. Am. J. Physiol. Endocrinol. Metab. 307, E469–E484.

Borner, T., Arnold, M., Ruud, J., Breit, S.N., Langhans, W., Lutz, T.A., Blomqvist, A., Riediger, T., 2017. Anorexia-cachexia syndrome in hepatoma tumour-bearing rats requires the area postrema but not vagal afferents and is paralleled by increased MIC-1/GDF15. Journal of cachexia, sarcopenia and muscle 8, 417–427.

Borner, T., Liberini, C.G., Lutz, T.A., Riediger, T., 2018. Brainstem GLP-1 signalling contributes to cancer anorexia-cachexia syndrome in the rat. Neuropharmacology 131, 282–290.

Braun, T.P., Marks, D.L., 2015. The regulation of muscle mass by endogenous glucocorticoids. Front. Physiol. 6, 12.

Braun, T.P., Grossberg, A.J., Krasnow, S.M., Levasseur, P.R., Szumowski, M., Zhu, X.X., Maxson, J.E., Knoll, J.G., Barnes, A.P., Marks, D.L., 2013. Cancer- and endotoxin-induced cachexia require intact glucocorticoid signaling in skeletal muscle. Faseb. J. : official publication of the Federation of American Societies for Experimental Biology 27, 3572–3582.

Broadwell, R.D., Sofroniew, M.V., 1993. Serum proteins bypass the blood-brain fluid barriers for extracellular entry to the central nervous system. Exp. Neurol. 120, 245–263.

Burfeind, K.G., Michaelis, K.A., Marks, D.L., 2016. The central role of hypothalamic inflammation in the acute illness response and cachexia. Semin. Cell Dev. Biol. 54, 42–52.

Chen, X., Wu, Y., Yang, T., Wei, M., Wang, Y., Deng, X., Shen, C., Li, W., Zhang, H., Xu, W., Gou, L., Zeng, Y., Zhang, Y., Wang, Z., Yang, J., 2016. Salidroside alleviates cachexia symptoms in mouse models of cancer cachexia via activating mTOR signalling. Journal of cachexia, sarcopenia and muscle 7, 225–232.

Cole, R.L., Sawchenko, P.E., 2002. Neurotransmitter regulation of cellular activation and neuropeptide gene expression in the paraventricular nucleus of the hypothalamus. J. Neurosci. : the official journal of the Society for Neuroscience 22, 959–969.

Deyoung, M.P., Horak, P., Sofer, A., Sgroi, D., Ellisen, L.W., 2008. Hypoxia regulates TSC1/2-mTOR signaling and tumor suppression through REDD1-mediated 14-3-3 shuttling. Gene Dev. 22, 239–251.

Dunn-Meynell, A.A., Le Foll, C., Johnson, M.D., Lutz, T.A., Hayes, M.R., Levin, B.E., 2016. Endogenous VMH amylin signaling is required for full leptin signaling and protection from diet-induced obesity. Am. J. Physiol. Regul. Integr. Comp. Physiol. 310, R355–R365.

Emmerson, P.J., Wang, F., Du, Y., Liu, Q., Pickard, R.T., Gonciarz, M.D., Coskun, T., Hamang, M.J., Sindelar, D.K., Ballman, K.K., Foltz, L.A., Muppidi, A., Alsina-Fernandez, J., Barnard, G.C., Tang, J.X., Liu, X., Mao, X., Siegel, R., Sloan, J.H., Mitchell, P.J., Zhang, B.B., Gimeno, R.E., Shan, B., Wu, X., 2017. The metabolic effects of GDF15 are mediated by the orphan receptor GFRAL. Nat. Med. 23, 1215–1219.

Fearon, K., Strasser, F., Anker, S.D., Bosaeus, I., Bruera, E., Fainsinger, R.L., Jatoi, A., Loprinzi, C., MacDonald, N., Mantovani, G., Davis, M., Muscaritoli, M., Ottery, F., Radbruch, L., Ravasco, P., Walsh, D., Wilcock, A., Kaasa, S., Baracos, V.E., 2011. Definition and classification of cancer cachexia: an international consensus, the Lancet. Oncology 12, 489–495.

Gilson, H., Schakman, O., Combaret, L., Lause, P., Grobet, L., Attaix, D., Ketelslegers, J. M., Thissen, J.P., 2007. Myostatin gene deletion prevents glucocorticoid-induced muscle atrophy. Endocrinology 148, 452–460.

Gu, W., Geddes, B.J., Zhang, C., Foley, K.P., Stricker-Krongrad, A., 2004. The prolactin-releasing peptide receptor (GPR10) regulates body weight homeostasis in mice. J. Mol. Neurosci. : M. Inc. 22, 93–103.

Gullett, N.P., Mazurak, V.C., Hebbar, G., Ziegler, T.R., 2011. Nutritional interventions for cancer-induced cachexia. Curr. Probl. Canc. 35, 58–90.

Langhans, W., 2004. Anorexia during disease. In: Neurobiology of Food and Fluid Intake. Kluwer Academic Publishers, Boston, pp. 349–381.

Lee, Y., Yang, S.P., Soares, M.J., Voogt, J.L., 2000. Distribution of prolactin-releasing peptide mRNA in the rat brain. Brain Res. Bull. 51, 171–176.

Liposits, Z., Sherman, D., Phelix, C., Paull, W.K., 1986. A combined light and electron microscopic immunocytochemical method for the simultaneous localization of multiple tissue antigens. Tyrosine hydroxylase immunoreactive innervation of corticotropin releasing factor synthesizing neurons in the paraventricular nucleus of the rat. Histochemistry 85, 95–106.

Liu, C.-M., Yang, Z., Liu, C.-W., Wang, R., Tien, P., Dale, R., Sun, L.-Q., 2008. Myostatin antisense RNA-mediated muscle growth in normal and cancer cachexia mice. Gene Ther. 15, 155–160.

Lutz, T.A., 2010. The role of amylin in the control of energy homeostasis. Am. J. Physiol. Regul. Integr. Comp. Physiol. 298, R1475–R1484.

Maletínská, L., Nagelová, V., Tichá, A., Zemenová, J., Pirník, Z., Holubová, M., Špolcová, A., Mikulášková, B., Blechová, M., Sýkora, D., Lacinová, Z., Haluzík, M., Železná, B., Kuneš, J., 2015. Novel lipidized analogs of prolactin-releasing peptide have prolonged half-lives and exert anti-obesity effects after peripheral administration. Int. J. Obes. 39, 986–993.

Maniscalco, J.W., Zheng, H., Gordon, P.J., Rinaman, L., 2015. Negative energy balance blocks neural and behavioral responses to acute stress by "silencing" central glucagon-like peptide 1 signaling in rats. J. Neurosci. 35, 10701–10714.

Mcnamara, M.J., Alexander, H.R., Norton, J.A., 1992. Cytokines and their role in the pathophysiology of cancer cachexia. J. Parenter. Enteral Nutr. 16, 50S–55S.

Mera, T., Fujihara, H., Kawasaki, M., Hashimoto, H., Saito, T., Shibata, M., Saito, J., Oka, T., Tsuji, S., Onaka, T., Ueta, Y., 2006. Prolactin-releasing peptide is a potent mediator of stress responses in the brain through the hypothalamic paraventricular nucleus. Neuroscience 141, 1069–1086.

Mochiduki, A., Takeda, T., Kaga, S., Inoue, K., 2010. Stress response of prolactin-releasing peptide knockout mice as to glucocorticoid secretion. J. Neuroendocrinol. 22, 576–584.

Nayak, S., Herzog, R.W., 2010. Progress and prospects: immune responses to viral vectors. Gene Ther. 17, 295–304.

Paxinos, G., Watson, C., 2007. The Rat Brain in Stereotaxic Coordinates, sixth ed. Elsevier Academic Press.

Pigna, E., Berardi, E., Aulino, P., Rizzuto, E., Zampieri, S., Carraro, U., Kern, H., Merigliano, S., Gruppo, M., Mericskay, M., Li, Z., Rocchi, M., Barone, R.,

Macaluso, F., Di Felice, V., Adamo, S., Coletti, D., Moresi, V., 2016. Aerobic exercise and pharmacological treatments counteract cachexia by modulating autophagy in colon cancer. Sci. Rep. 6, 26991.
Puppa, M.J., Gao, S., Narsale, A.A., Carson, J.A., 2014. Skeletal muscle glycoprotein 130's role in Lewis lung carcinoma-induced cachexia. Faseb. J.: off.pub.Fed Am.Soc. Exp.Bio 28, 998–1009.
Riediger, T., 2012. The receptive function of hypothalamic and brainstem centres to hormonal and nutrient signals affecting energy balance. Proc. Nutr. Soc. 71.
Rodriguez, J., Vernus, B., Chelh, I., Cassar-Malek, I., Gabillard, J.C., Hadj Sassi, A., Seiliez, I., Picard, B., Bonnieu, A., 2014. Myostatin and the skeletal muscle atrophy and hypertrophy signaling pathways. Cell. Mol. Life Sci. 71, 4361–4371.
Roland, B.L., Sutton, S.W., Wilson, S.J., Luo, L., Pyati, J., Huvar, R., Erlander, M.G., Lovenberg, T.W., 1999. Anatomical distribution of prolactin-releasing peptide and its receptor suggests additional functions in the central nervous system and periphery. Endocrinology 140, 5736–5745.
Ruud, J., Blomqvist, A., 2007. Identification of rat brainstem neuronal structures activated during cancer-induced anorexia. J. Comp. Neurol. 504, 275–286.
Sadeghi, M., Keshavarz-Fathi, M., Baracos, V., Arends, J., Mahmoudi, M., Rezaei, N., 2018. Cancer cachexia: diagnosis, assessment, and treatment. Crit. Rev. Oncol.-Hematol. 127, 91–104.
Saxton, R.A., Sabatini, D.M., 2017. mTOR signaling in growth, metabolism, and disease. Cell 168, 960–976.
Schakman, O., Kalista, S., Barbé, C., Loumaye, A., Thissen, J., 2013. Glucocorticoid-induced skeletal muscle atrophy. Int. J. Biochem. Cell Biol. 45, 2163–2172.
Seal, L.J., Small, C.J., Dhillo, W.S., Kennedy, A.R., Ghatei, M.A., Bloom, S.R., 2002. Prolactin-releasing peptide releases corticotropin-releasing hormone and increases plasma adrenocorticotropin via the paraventricular nucleus of the hypothalamus. Neuroendocrinology 76, 70–78.
Tachibana, T., Sakamoto, T., 2014. Functions of two distinct "prolactin-releasing peptides" evolved from a common ancestral gene. Front. Endocrinol. 5, 170.
Takayanagi, Y., Matsumoto, H., Nakata, M., Mera, T., Fukusumi, S., Hinuma, S., Ueta, Y., Yada, T., Leng, G., Onaka, T., 2008. Endogenous prolactin-releasing peptide regulates food intake in rodents. J. Clin. Invest. 118, 4014–4024.
Taxman, D.J., Moore, C.B., Guthrie, E.H., Huang, M.T.-H., 2010. Short hairpin RNA (shRNA): design, delivery, and assessment of gene knockdown. CliftonN. J.. In: Methods in Molecular Biology, 629, pp. 139–156.
Taylor, W.E., Bhasin, S., Artaza, J., Byhower, F., Azam, M., Willard, D.H., Kull, F.C., Gonzalez-Cadavid, N., 2001. Myostatin inhibits cell proliferation and protein synthesis in C2 C12 muscle cells. Am. J. Physiol. Endocrinol. Metab. 280, E221–E228.
van Norren, K., Dwarkasing, J.T., Witkamp, R.F., 2017. The role of hypothalamic inflammation, the hypothalamic-pituitary-adrenal axis and serotonin in the cancer anorexia-cachexia syndrome. Curr. Opin. Clin. Nutr. Metab. Care 20, 396–401.
Vanhoutte, G., van de Wiel, M., Wouters, K., Sels, M., Bartolomeeussen, L., De Keersmaecker, S., Verschueren, C., De Vroey, V., De Wilde, A., Smits, E., Cheung, K. J., De Clerck, L., Aerts, P., Baert, D., Vandoninck, C., Kindt, S., Schelfhaut, S., Vankerkhoven, M., Troch, A., Ceulemans, L., Vandenbergh, H., Leys, S., Rondou, T., Dewitte, E., Maes, K., Pauwels, P., De Winter, B., Van Gaal, L., Ysebaert, D., Peeters, M., 2016. Cachexia in cancer: what is in the definition? BMJ Open Gastroenterology 3, e000097.
Villars, F., Pietra, C., Giuliano, C., Lutz, T., Riediger, T., 2017. Oral treatment with the ghrelin receptor agonist HM01 attenuates cachexia in mice bearing colon-26 (C26) tumors. Int. J. Mol. Sci. 18, 986.
Wang, H., Kubica, N., Ellisen, L.W., Jefferson, L.S., Kimball, S.R., 2006. Dexamethasone represses signaling through the mammalian target of rapamycin in muscle cells by enhancing expression of REDD1. J. Biol. Chem. 281, 39128–39134.
White, J.P., Baynes, J.W., Welle, S.L., Kostek, M.C., Matesic, L.E., Sato, S., Carson, J.A., 2011. The regulation of skeletal muscle protein turnover during the progression of cancer cachexia in the Apc(Min/+) mouse. PloS One 6, e24650.
Zhao, J., Zhai, B., Gygi, S.P., Goldberg, A.L., 2015. mTOR inhibition activates overall protein degradation by the ubiquitin proteasome system as well as by autophagy. Proc. Natl. Acad. Sci. Unit. States Am. 112, 15790–15797.
Zheng, H., Stornetta, R.L., Agassandian, K., Rinaman, L., 2015. Glutamatergic phenotype of glucagon-like peptide 1 neurons in the caudal nucleus of the solitary tract in rats. Brain Struct. Funct. 220, 3011–3022.